Molecular Crystals and Liquid Crystals

Publication details, including instructions for authors and subscription information:
http://www.tandfonline.com/loi/gmcl20

Effect of Molecular Chain Orientation on Carrier Transport and Trapping in Polymer Blends

V. Kažukauskas [a] , V. Čyras [a] , L. Sicot [b] & C. Sentein [b]

[a] Department of Semiconductor Physics and Institute of Materials Science and Applied Research, Vilnius University, Vilnius, Lithuania

[b] DRT-LITEN-DSEN-GENEC-L2C, Gif-sur-Yvette, France

Version of record first published: 23 Aug 2006

To cite this article: V. Kažukauskas, V. Čyras, L. Sicot & C. Sentein (2006): Effect of Molecular Chain Orientation on Carrier Transport and Trapping in Polymer Blends, Molecular Crystals and Liquid Crystals, 447:1, 155/[473]-166/[484]

To link to this article: http://dx.doi.org/10.1080/15421400500387122

Mol. Cryst. Liq. Cryst., Vol. 447, pp. 155/[473]–166/[484], 2006

ISSN: 1542-1406 print/1563-5287 online
DOI: 10.1080/15421400500387122

Taylor & Francis
Taylor & Francis Group

Effect of Molecular Chain Orientation on Carrier Transport and Trapping in Polymer Blends

V. Kažukauskas
V. Čyras
Department of Semiconductor Physics and Institute of Materials Science and Applied Research, Vilnius University, Vilnius, Lithuania

L. Sicot
C. Sentein
DRT-LITEN-DSEN-GENEC-L2C, Gif-sur-Yvette, France

Carrier transport and trapping effects, as they are influenced by molecular chain orientation, were investigated by Thermally Stimulated Currents (TSC) and Current-Voltage (IV) characteristics in the samples of poly(9-vinylcarbazole) (PVK) doped with 30% wt 4-dibutylamino-4′-nitrostilbene (DBANS). The orientation of DBANS, diode-like molecules, was performed by electric field above the glass transition temperature. We demonstrate that the orientation of polar molecules causes significant changes both in IV dependencies and the TSC spectra. Changes of the TSCs induced by orientation were expressed best in the temperature range of 280–290 K. They could be attributed to the thermally activated process with activation energy of about 0.38 eV.

Keywords: carrier transport and trapping; molecular chain orientation; polymers PVK and DBANS

PACS: 72.80.Le; 73.50.Gr; 73.61.Ph; 81.40.Rs

The authors would like to acknowledge partial financial support by the European Commission (FP6 MOLYCELL project, contract No SES6-CT-2003-502783), the Lithuanian State Science and Studies Foundation (project No T-29/05) and bilateral support by the EGIDE agency (France) and the Department of Science and Higher Education of the Ministry of Education and Science (Lithuania) within the "Gilibert" project.

Address correspondence to V. Kažukauskas, Department of Semiconductor Physics and Institute of Materials Science and Applied Research of Vilnius University, Saulėtekio 9, bldg. 3, LT-10222 Vilnius, Lithuania. E-mail: vaidotas.kazukauskas@ff.vu.lt

INTRODUCTION

Organic electronics is one of the promising and fast developing fields. Particularly, organic-based photovoltaics (PV) can give unique advantages over the traditional silicon based approach from the point of view of production simplicity and convenience. The components used for organic PV devices are potentially cheap, non-toxic, widely available and can be tailored to suit specific needs (e.g., for selective light harvesting). Manufacturing of organic PV devices is straightforward since low temperature fabrication steps can be used such as screen-printing, ink-jet printing and solution spraying. As compared to present (inorganic) PV technologies, the energy and equipment requirements for producing organic PV devices are thus only minor. Furthermore, such deposition routes are compatible with non-heat resistant substrates such as plastics, allowing high throughput reel-to-reel manufacturing of flexible and lightweight PV modules by integrating well-known thermoplastic processing technologies. Organic photovoltaics could thus become a major technology for sustainable electricity generation in the long term.

Organic solar cells might promise a strong cost reduction if fast improvements of the power efficiency and the lifetime can be achieved. To build up efficient photovoltaic cells, a rectifying junction is necessary to effectively spatially separate the photogenerated carriers. One approach to realize such a junction extended over the whole device thickness may be the use of molecular rectification in an oriented amorphous polymer layer incorporating polar molecules. In such layer an internal electric field is introduced and stored and therefore the structure behaves as a distributed homojunction within a single polymer thin-film [1,2]. This new principle enables one to avoid the necessity of the deposition of several layers, as in the cases of the Schottky or *p-n* junctions. Moreover bulk of the device could be used more effectively as charge separation occurs in the whole layer. The principle relies on the intrinsic polar nature of organic molecules, and therefore it cannot be readily applied to inorganic semiconductors which are built from spherical atoms, polarity being a crystal-cell property. Oriented diode-like molecules – the so-called push-pull molecules used in second-order nonlinear optics [3] – are contained inside a polymer binder. They induce a rectifying effect behaving as a distributed homojunction within a single polymer thin-film [1]. Orientation of dopant molecules can be achieved by application of a static electric field through the polymer film, while heating near the glass transition temperature. Molecular orientation is characterized by an order parameter $\langle \cos\theta \rangle$ [4]. Experimentally it was demonstrated that the

current-voltage characteristics of oriented Disperse Red 1 (DR1) (4-(N-(2-hydroxyethyl)-N-ethyl)-amino-4′-nitroazobenzene) films attached onto poly(methyl methacrylate) (PMMA) become strongly asymmetric [5]. Moreover, molecular order can be controlled using second harmonic generation (SHG). A new method – voltage-dependent SHG – was proposed to probe the internal field induced in the structure. It was called SEFISHG (Solid Electric Field Induced Second Harmonic Generation) [6] and was demonstrated to be related to the induced rectification behavior [7].

On the other hand, device efficiency also depends on carrier transport properties, which are given by carrier mobility and trapping. Engineering of macroscopic devices is necessarily based not only on the technological advances and skills, but, in the same amount, on the purposeful control of carrier flows, which in their turn are given by microscopic material properties. Both carrier mobility and trapping effects can be foreknown to depend in different manner on molecular chain type and structure and on their orientation too. Usually in conjugated polymers charges are severely trapped by defect states. This results in reduced electron or hole mobility and imbalance of electron and hole flows, the equality of which is of primary importance for many modern applications of polymer materials, e.g., light-emitting and harvesting devices. Increase of the carrier mobility after the orientation of diode-like molecules was evidenced by the Time of Flight (TOF) method [1]. In this article we will analyze effect of molecular orientation on charge carrier transport and trapping in the samples of poly(9-vinylcarbazole) (PVK) doped with 30% wt 4-dibutylamino-4′-nitrostilbene (DBANS).

SAMPLES AND EXPERIMENT

Effect of the molecular chain orientation on thermally stimulated carrier transport was investigated by Thermally Stimulated Currents (TSC) and Current-Voltage (IV) characteristics in the samples of PVK (poly(9-vinylcarbazole)) blended with 30% wt DBANS (4-dibutylamino-4′-nitrostilbene). The choice of the DBANS molecule was motivated by the facts that it possesses, as DR1, a large ground state dipole moment, which is necessary for the efficient DC-field orientation, and is less sensible to disorientation under light illumination than azobenzene dyes. PVK was used because of its high glass transition temperature ($T_g \cong 200^{\circ}$C) which enables more stable orientation as compared to polymers like poly(3-alkylthiophenes) (P3AT) or poly (phenylen vinylen)s (PPVs), used in photovoltaic cells. On the other hand PVK is more conductive than poly(methyl methacrylate) (PMMA).

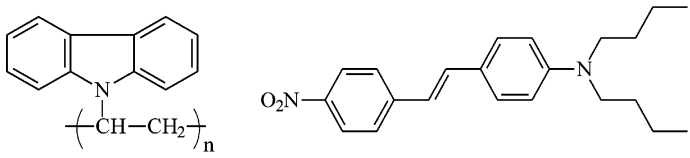

a) b)

FIGURE 1 Molecular structures of the blend constituents: a) PVK (poly (9-vinylcarbazole)), b) DBANS (4-dibutylamino-4′-nitrostilbene).

The polymer structures are presented in Figure 1. Samples were prepared by the spin coating and were 1.3 μm thick. The blend was deposited on an ITO-coated glass substrate. The samples were provided with evaporated Al contacts on the top. The molecular chain orientation was performed at 394 K by applying 105 V voltage. The reverse bias was applied to create polarization field oriented in the forward direction and vice versa. The bias was maintained while cooling the samples down to the room temperature. The TSCs and the dark currents were measured after the white-light excitation and without excitation at liquid nitrogen temperature, respectively. During the heating a constant heating rate of 10 K/min was maintained. After each measurement cycle the chain orientation procedure was repeated.

METHODICAL BACKGROUND

To quantitatively analyze the trap parameters by fitting the experimental curves we used a TSC model proposed in [8], as it is described in detail in [9,10]. The kinetics of carrier density at the traps may be described as [8]:

$$\frac{dn_t}{dT} = -\frac{f_t n_t}{\beta}\exp\left(-\frac{E_t}{kT}\right), \tag{1}$$

here n_t is carrier density at traps with an activation energy E_t, T is temperature, β is a heating rate, k is Boltzmann constant, f_t is a carrier attempt-to-escape frequency. Assuming that f_t is temperature independent and the initial condition is $n_t(T_0) = n_{t0}$, an approximate solution of Eq. (1) can be obtained, that can further be used to calculate the current caused by thermally generated carriers [8]:

$$I = \frac{1}{2}eLAf_t n_{t0}\exp\left[-\frac{E_t}{kT} - \frac{f_t kT^2}{\beta(E_t + kT)}\exp\left(-\frac{E_t}{kT}\right)\right], \tag{2}$$

here e is elementary charge, L is a layer thickness, A is a sample area. Equation (2) can be used to model the single TSC peaks, by choosing the fitting parameters E_t , n_{t0}, and f_t.

Unfortunately, by interpreting experimental results usually the problem arises that no theory adequately explains various transport phenomena in polymers, particularly the electric field and temperature dependencies of drift mobility [11–16]. The most frequently used approaches refer to hopping transport character in disordered organic solids and are based either on a modified Poole-Frenkel (PF) model [12] or a Gaussian disorder model (GDM) [17]. The latter was later extended to include correlation effects [18–20]. In the Poole-Frenkel model the mobility can be described as a field and temperature assisted detrapping process of a carrier from the Coulomb potential of a charged trap. The mobility is given by [12]:

$$\mu = \mu_0 \exp\left[-\frac{E_0 - \alpha F^{1/2}}{kT_{eff}}\right] \tag{3}$$

with

$$1/T_{eff} = 1/T - 1/T_R, \tag{4}$$

where F is an electric field strength, E_0 is an activation energy of the carrier transport at zero electric field, and T_R is the empirical reference temperature at which mobility is supposed to be known.

In the GDM model charge transport in disordered organic conductors is supposed to proceed by means of hopping in a Gaussian site-energy distribution. This density of states (DOS) reflects the energetic spread in the charge transporting levels of chain segments due to fluctuation in conjugation lengths and structural disorder. Within the Gaussian disorder model the mobility is given by [17]:

$$\mu(F,T) = \mu_\infty \exp\left[-\left(\frac{2\sigma}{3kT}\right)^2\right] \exp\left\{C\left[\left(\frac{\sigma}{kT}\right)^2 - \Sigma^2\right]\sqrt{F}\right\} \tag{5}$$

This equation was derived from Monte-Carlo simulations of the hopping processes of charge carriers in a material with energetic (σ) and positional disorder (Σ) described by Gaussian distribution functions. μ_∞ is the high temperature limit of the mobility and C is a specific parameter that is obtained from the simulations as $C = 2.9 \times 10^{-4}$ $(\mathrm{cm/V})^{1/2}$.

Behavior approximated by both these empirical equations has been observed in many materials. Experimentally, the main difference

between both models is the temperature dependence. A consequence of hopping in a Gaussian DOS is the non-Arrhenius behavior of the mobility [17]. Nevertheless within the limited temperature range it is practically impossible to discriminate between both dependencies. Furthermore, the simulations of the GDM reproduced the $\ln(\mu) \sim \sqrt{F}$ dependence only in a narrow field range at high fields (10^8 V/m) [16]. Apart from that, both models require many parameters that can be used to fit the experimental data, depending on the preferred model. This causes that actually both approaches can be applied to fit experimental results, basing on the chosen physical mechanism, that in many cases is not known *a priori* [21]. Therefore there are rare examples where a clear distinction between the two models has been possible [22].

Moreover, in hopping systems the thermally activated mobility behavior can cause appearance of the thermally stimulated current maxima [23]. Therefore in general it is difficult to make a final decision if the results are caused by the change of carrier concentration or their mobility. On the other hand in the latter case TSC maxima should demonstrate an expressed dependence on the heating rate and applied electric field [23].

RESULTS AND DISCUSSION

First of all the effect of molecular orientation was tested by investigating the Current-Voltage (IV) characteristics. To avoid a clearly expressed long living sample polarization by high applied electric fields (as it was also observed in, e.g., MEH-PPV and reported in more detail in [10,24]), measurements were always started from zero fields, and voltage was increased in small steps of 10 mV allowing sufficient relaxation time between the steps. Under such conditions we did not observe any influence of the molecular orientation at 300 K temperature. On the other hand at lower temperatures below about 250 K an expressed effect of the molecular orientation was identified, as it is demonstrated in Figure 2. It is clearly seen that if molecules were oriented in forward direction, i.e., their dipole field to be of the same direction as an external electrical field, creating forward current, a built-in electric field was created in the sample. This field caused the current flow in an opposite direction at low values of the applied reverse bias up to about –3.3 V. Similarly, upon reverse orientation, the built-in field could be compensated by applying about 3.5 V forward bias. Characteristically the observed behavior can be attributed primarily to the ohmic conduction of the layer volume itself. Meanwhile, e.g., contact effects make only minor influence. It is evidenced

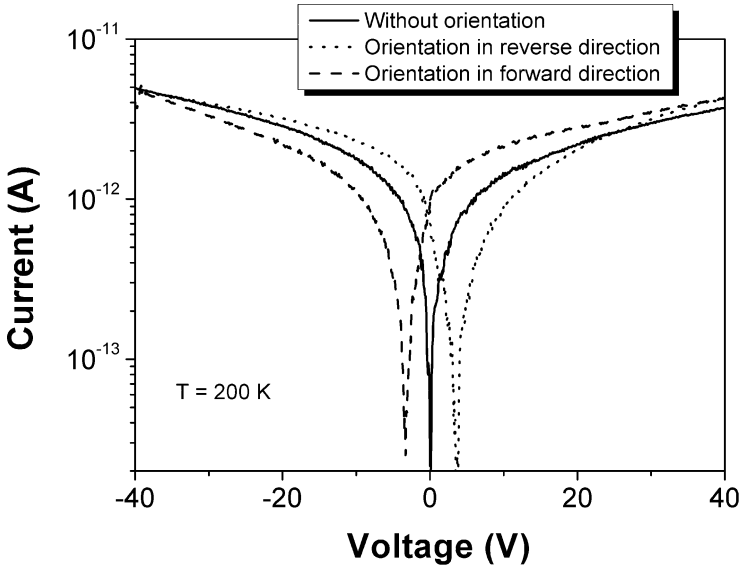

FIGURE 2 Current-voltage characteristics, measured at 200 K, depending on the molecular orientation of the sample. Note that here and further the absolute current values are plotted.

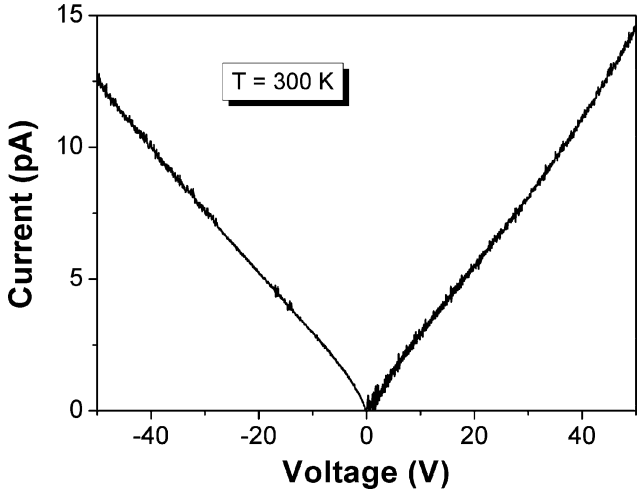

FIGURE 3 Current-voltage characteristics in linear representation, measured at 300 K.

by Figure 3, in which IV curves are presented at 300 K in linear scaling. It can be seen that at least up to the electric field strength of 4×10^5 V/cm the sample demonstrates ohmic behavior with the sample resistance of about $(3.6 - 4.2) \times 10^{12}\,\Omega$ and specific resistivity of about $(1.3 - 1.7) \times 10^{16}\,\Omega$cm. This does not enable evaluation nor of contact parameters, nor of carrier mobility, as it would be possible in case of other prevailing current-limiting mechanisms, e.g., thermionic emission over the contact potential barrier, Fowler-Nordheim tunneling or space-charge-limited currents.

Clear effect of the molecular orientation could be observed also in the Thermally Stimulated Current spectra, as is presented in Figure 4. In all the cases marked differences are induced by the light excitation in the thermally stimulated regime, as compared to the unexcited dark currents. As far as PVK has an energy gap of about 6 eV, and therefore can hardly be excited by the white light, the observed excitation effects could be attributed to DBANS. The TSCs had the effective thermal activation energies of about 0.037 eV in the temperature region of 166–240 K. Such small values are most probably caused not by carrier generation from traps, but rather by the thermally stimulated mobility growth. This means that mobility can be varied by light excitation. Changes of the TSCs induced by orientation

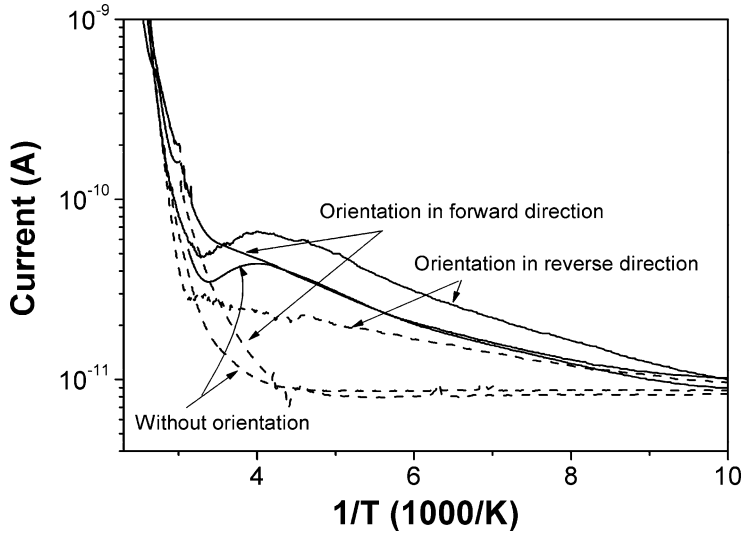

FIGURE 4 Thermally stimulated currents (solid lines) and dark currents (dashed curves) depending on the molecular orientation, as indicated on Figure.

were expressed best in the temperature range of 260–290 K. In the unoriented and oriented in reverse direction samples a clear current dip appears in this region in contrast to the samples oriented in the forward direction.

As can be seen from Figure 4, near the room temperature higher conductivity is assured upon excitation after the orientation in forward direction, what can offer increase of the light-harvesting device efficiency. Therefore to analyze differences between this case and unoriented sample, we modeled the experimental dependencies by taking into account thermal carrier generation from the trap states as well as their mobility changes given by the Gaussian disorder (GDM) and Poole-Frenkel (PF) approximations according to Eqs. (2)–(5). Results are presented in Figure 5. Nearby the curves indicating carrier thermal generation, the trap parameters, i.e., their thermal activation energy and initial filling are presented. Values used for the calculation of mobility effect are as follows. Poole-Frenkel model: $\mu_0 = 5.40\times\ 10^{-11}\,\mathrm{cm^2/Vs}$, $E_0 = 0.152\,\mathrm{eV}, T_R = 1000\,\mathrm{K}, \alpha = 1.95 \times 10^{-4}$ $\mathrm{eV(cm/V)^{1/2}}$. Gaussian disorder model: $\mu_\infty = 1.25 \times 10^{-7}\,\mathrm{cm^2/Vs}$, $\Sigma = 4.9, \sigma = 0.039\,\mathrm{eV}, C = 5.00 \times 10^{-4}\,\mathrm{(cm/V)^{1/2}}$. It is necessary to note that these values used for mobility calculations are only indicative ones, because very similar trends of the curves could be obtained by different sets of parameters. As it is seen from Figure 5, the important issue is that most fitting parameters were kept unchanged in both cases, evidencing that orientation induces only very definite changes in the thermally stimulated behavior. These changes relate to the varying influence of the thermally stimulated process with the effective activation energy of about 0.38 eV. This peak appears on the background of the other thermally stimulated process with even higher activation energy, therefore it could be associated not only with thermal carrier generation from the trap state, but also with mobility change.

Notably, the reversely oriented sample exhibits in Figure 4 the TSC and the dark current both running significantly higher than in other cases. This indicates a noticeably increasing effect of the thermally stimulated mobility. Unfortunately, usually orientation in reverse direction did not give well reproducible results in contrast to the other two cases, therefore additional investigations are necessary to explain its nature. One of the reasons of the steeper mobility increase with temperature could be the necessity for the carriers to overcome higher potential barriers induced by the reverse orientation of molecules.

Above about 310 K the current increase begins with the activation energy of about 0.9 eV. Probably it can be attributed to the carriers thermally excited over the potential barrier at one of the contacts.

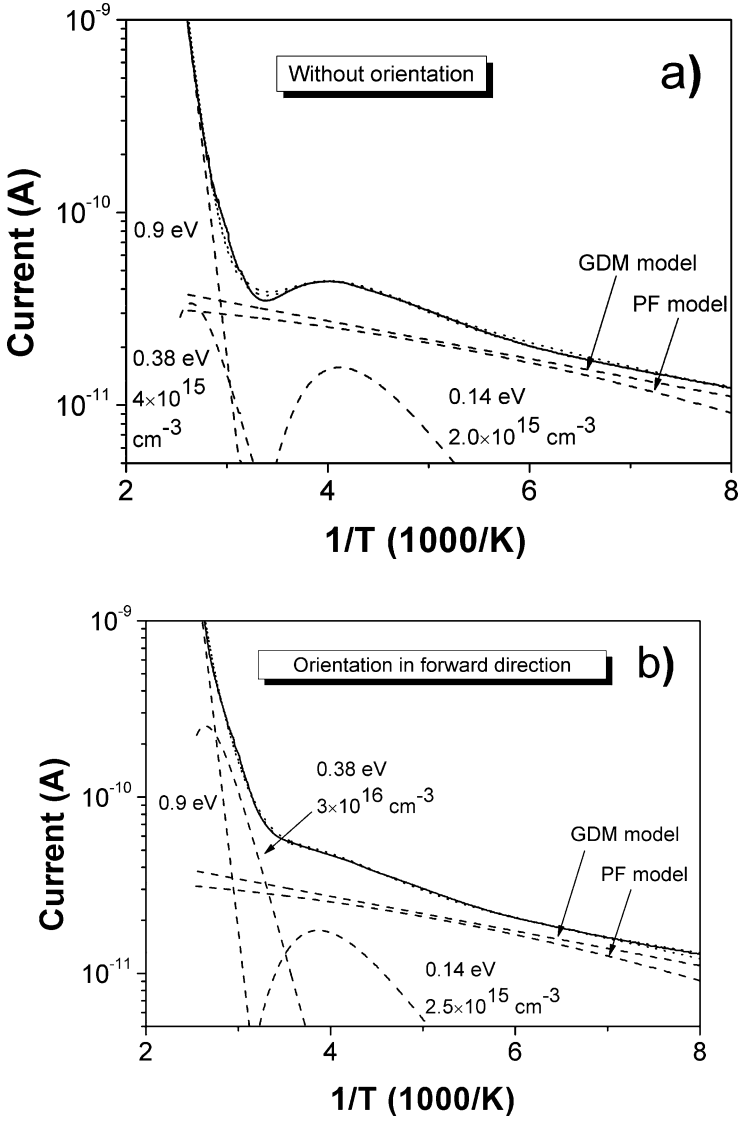

FIGURE 5 Fit of the TSCs measured a) without orientation, b) after the orientation in forward direction. Experimental curves are presented by solid lines, the fitting curves are plotted by dotted lines, and influences of different thermally activated processes are plotted by dashed lines. Nearby the curves representing carrier thermal generation, trap parameters (thermal activation energy and initial trap filling) are indicated.

SUMMARY AND CONCLUSIONS

Carrier transport and trapping effects, as they are influenced by molecular chain orientation, were investigated by Thermally Stimulated Currents and Current-Voltage characteristics in the samples of poly(9-vinylcarbazole) (PVK) doped with 30% wt 4-dibutylamino-4′-nitrostilbene (DBANS). The orientation of molecules was performed by electric field at 394 K. The reverse bias was applied to create polarization field oriented in the forward direction and vice versa. The TSCs and the dark currents were measured after the white-light excitation at liquid nitrogen temperature and without excitation, respectively. We demonstrated that the molecular chain orientation induces significant changes both in IV dependencies below about 250 K temperature and the TSC spectra. Well expressed differences between the TSCs and dark currents were evidenced experimentally, depending on the direction of the orientation of polar DBANS molecules. The TSCs could be modeled by taking into account mobility variation according to the Gaussian disorder and Poole-Frenkel approximations as well as carrier thermal generation from traps. In the temperature region of 166–240 K the effective thermal activation energies of TSC curves were about 0.037 eV. Such small values are most probably caused not by carrier generation from traps, but rather by the thermally stimulated mobility growth. This means that mobility can be varied by light excitation. Changes of the TSCs induced by orientation were expressed best in the temperature range of 280–290 K. The numerical fitting revealed that they could be attributed to the thermally activated process with activation energy of about 0.38 eV. Above about 310 K the current increase took place with an activation energy of 0.9 eV, that could be caused by the carriers thermally excited over the potential barrier at one of the contacts.

REFERENCES

[1] Sentein, C., Fiorini, C., Lorin, A., & Nunzi, J.-M. (1997). *Advanced Materials*, *9*(10), 809.
[2] Sentein, C., Fiorini, C., Lorin, A., Nunzi, J.-M., Raimond, P., & Sicot, L. (1999). *Synthetic Metals*, *102*, 989.
[3] Oudar, J. L. (1977). *J. Chem. Phys.*, *67*, 446.
[4] Singer, K. D., Kuzyk, M. G., & Sohn, J. E. (1987). *J. Opt. Soc. Am. B*, *4*, 968.
[5] Sentein, C., Fiorini, C., Lorin, A., & Nunzi, J.-M. (1997). *Synthetic Metals*, *91*, 81.
[6] Sentein, C., Fiorini, C., Lorin, A., Sicot, L., & Nunzi, J.-M. (1998). *Optical Materials*, *9*, 316.
[7] Sicot, L., Fiorini, C., Lorin, A., Raimond, P., Sentein, C., & Nunzi, J.-M. (2000). *Solar Energy Materials & Solar Cells*, *63*, 49.
[8] Simmons, J. G. & Taylor, G. W. (1972). *Phys. Rev. B*, *5*, 1619.

[9] Kavaliauskienė, G., Kažukauskas, V., Rinkevičius, V., Storasta, J., Vaitkus, J. V., Bates, R., O'Shea, V., & Smith, K. M. (1999). *Appl. Phys. A*, *69*, 415.
[10] Kažukauskas, V. (2004). *Semicond. Sci. Technol.*, *19*, 1373.
[11] Kepler, R. G., Beeson, P. M., Jacobs, S. J., Anderson, R. A., Sinclair, M. B., Valencia, V. S., & Cahill, P. A. (1995). *Appl. Phys. Lett.*, *66*, 3618.
[12] Gill, W. D. (1972). *J. Appl. Phys.*, *43*, 5033.
[13] Borsenberger, P. M. & Weiss, D. W. (Eds.) (1993). *Organic Photoreceptors for Imaging Systems*, Dekker: New York.
[14] Abkowitz, M. A. (1992). *Philos. Mag. B*, *65*, 817.
[15] Schein, L. B. (1992). *Philos. Mag. B*, *65*, 795.
[16] Blom, P. W. M. & Vissenberg, M. C. J. M. (2000). *Materials Science and Engineering*, *27*, 53.
[17] Baessler, H. (1993). *Phys. Stat. Solidi (b)*, *175*, 15.
[18] Dunlap, D. H., Parris, P. E., & Kenkre V. M. (1996). *Phys. Rev. Lett.*, *77*, 542.
[19] Novikov, S. V., Dunlap, D. H., Kenkre, V. M., Parris, P. E., & Vannikov, A. V. (1998). *Phys Rev. Lett.*, *81*, 4472.
[20] Dunlap, D. H., Kenkre, V. M., & Parris, P. E. (1999). *J. Imag. Sci. Technol.*, *43*, 437.
[21] Bruetting, W., Berleb, S., & Mueckl, A. G. (2001). *Organic Electronics*, *2*, 1.
[22] Hertel, D., Baessler, H., Scherf, U., & Hoerhold, H. H. (1999). *J. Chem. Phys.*, *110*, 9214.
[23] Chen, I. (1976). *J. Appl. Phys.*, *47*, 2988.
[24] Kažukauskas, V. (2003). *Proc. SPIE*, *5122*, 163.